Domain growth in Ising systems with quenched disorder

Raja Paul,[1] Sanjay Puri,[2] and Heiko Rieger[1]
[1]*Theoretische Physik, Universität des Saarlandes, 66041 Saarbrücken, Germany*
[2]*School of Physical Sciences, Jawaharlal Nehru University, New Delhi 110067, India*
(Received 24 February 2005; published 30 June 2005)

We present results from extensive Monte Carlo (MC) simulations of domain growth in ferromagnets and binary mixtures with quenched disorder. These are modeled by the random-bond Ising model and the dilute Ising model with either nonconserved (Glauber) spin-flip kinetics or conserved (Kawasaki) spin-exchange kinetics. In all cases, our MC results are consistent with power-law growth with an exponent $\theta(T,\epsilon)$ which depends on the quench temperature T and the disorder amplitude ϵ. Such exponents arise naturally when the coarsening domains are trapped by energy barriers that grow logarithmically with the domain size. Our MC results show excellent agreement with the predicted dependence of $\theta(T,\epsilon)$.

DOI: 10.1103/PhysRevE.71.061109 PACS number(s): 05.40.−a, 64.75.+g

I. INTRODUCTION

Consider a binary mixture that is homogeneous at high temperatures. This system becomes thermodynamically unstable if it is quenched below the critical temperature. The subsequent evolution of the system is characterized by the formation and growth of domains enriched in either component. These domains have a characteristic size $R(t)$, which grows with time. The domain growth law $R(t)$ vs t depends on general system properties, e.g., the nature of conservation laws governing the order parameter evolution, the presence of hydrodynamic velocity fields, the presence of quenched or annealed disorder, etc. There is a good understanding of the growth laws for pure and isotropic systems [1–4]. For the case with nonconserved order parameter, e.g., ordering of a magnet into up and down phases, the system obeys the Lifshitz-Cahn-Allen (LCA) growth law $R(t)\sim t^{1/2}$. For the case with conserved order parameter, e.g., diffusion-driven phase separation of an AB mixture into A-rich and B-rich phases, the system obeys the Lifshitz-Slyozov (LS) growth law $R(t)\sim t^{1/3}$.

Recent interest in domain growth problems has focused on modeling and understanding the effects of various experimentally relevant features. In this context, an important set of analytical and numerical studies has investigated coarsening in systems with quenched disorder [5–13]. In general, one expects that trapping of domain boundaries by disorder sites will result in slower domain growth. However, these studies were unable to clarify the nature (or even existence) of a universal growth law. In a recent letter [14], we have reconsidered this problem through comprehensive Monte Carlo (MC) simulations of kinetic Ising models. In our letter, we presented MC results for ordering in random magnets, modeled by the *random-bond Ising model* (RBIM) with nonconserved (Glauber) spin-flip kinetics. (In the RBIM, the presence of disorder is mimicked by randomizing the exchange coupling between spins.) In this paper, we present further results for coarsening in two classes of disordered systems

(a) The RBIM with conserved (Kawasaki) spin-exchange kinetics, which models phase separation in disordered binary mixtures.

(b) The *dilute Ising model* (DIM) with both nonconserved and conserved kinetics. The DIM is relevant in cases where disorder is introduced via either *bond dilution* or *site dilution*.

The results in this paper, in conjunction with those in our letter, constitute an understanding of domain growth in systems with quenched disorder. This paper is organized as follows. In Sec. II, we summarize arguments for growth laws in disordered systems. In Sec. III, we present results for the RBIM with conserved kinetics. In Sec. IV, we present results for the DIM with both nonconserved and conserved kinetics. Finally, Sec. V concludes this paper with a summary and discussion of our results.

II. GROWTH LAWS IN DISORDERED SYSTEMS

A. Nonconserved case

An important step toward understanding growth laws in nonconserved systems is due to Lai, Mazenko, and Valls (LMV) [15]. LMV proposed four classes of systems, determined by the dependence of the energy barrier on coarsening on the characteristic scale. The growth of domains is driven by a curvature-reduction mechanism as

$$\frac{dR}{dt}=\frac{a(R,T)}{R}, \tag{1}$$

where the diffusion constant $a(R,T)$ depends on the domain scale R and temperature T, in general. For pure systems, the diffusion constant is independent of the length scale, i.e., $a(R,T)=a_0$. The corresponding growth law is the LCA law $R(t)=(2a_0t)^{1/2}$.

Let us next consider systems with quenched disorder. At early times and small length scales, the growing domains are not affected by disorder $[a(R,T)\simeq a_0]$ and the growth law is the same as that for the pure case. At late times, the domains are trapped by disorder sites, creating a barrier (E_B) to domain growth. Then, the asymptotic dynamics is driven by thermal activation over disorder barriers with $a(R,t)\simeq a_0\exp(-\beta E_B)$, where $\beta=T^{-1}$ ($k_B=1$). For the bond-disordered case, Huse and Henley (HH) [5] argued that the

energy barrier scales as $E_B(R) \simeq \epsilon R^{\psi}$, where ϵ is the disorder strength. The barrier exponent ψ depends on the roughening exponent ζ and the pinning exponent χ as $\psi = \chi/(2-\zeta)$. Further, the roughening and pinning exponents are related as $\chi = 2\zeta + d - 3$, where d is the dimensionality. For power-law barriers, Eq. (1) yields an asymptotic growth law which is *logarithmic*, viz.,

$$R(t) \simeq \left[\frac{T}{\epsilon} \ln\left(\frac{t}{t_0} \right) \right]^{1/\psi},$$

$$t_0 \simeq \frac{1}{a_0 \psi} \left(\frac{T}{\epsilon} \right)^{2/\psi}. \tag{2}$$

We can reformulate the early-time and late-time behaviors as limiting cases of a crossover function:

$$R(t) = R_0(T,\epsilon) h\left(\frac{t}{t_0} \right), \tag{3}$$

where

$$R_0(T,\epsilon) = \left(\frac{T}{\epsilon} \right)^{1/\psi} \tag{4}$$

and

$$h(x) = \begin{cases} \left(\frac{2}{\psi} x \right)^{1/2}, & x \ll 1, \\ (\ln x)^{1/\psi}, & x \gg 1. \end{cases} \tag{5}$$

For $d=2$, $\zeta = 2/3$, and $\chi = 1/3$ [16,17], yielding $\psi = 1/4$. For $d=3$, a perturbative calculation gives $\psi \simeq 0.55$ [5]. There have been a number of numerical simulations [6–13] and experiments [18–20] which have attempted to test the HH scenario. However, to date, there is no clear confirmation of HH growth in the asymptotic regime. As a matter of fact, it is not even clear whether there is a universal law which characterizes the disorder-affected growth regime.

In recent work [14], we have reconsidered this problem via extensive MC simulations of the RBIM with nonconserved kinetics. Our results were consistent with power-law domain growth, but with a temperature- and disorder-dependent exponent. Similar observations have been made in experiments on coarsening in disordered systems [18–20]. Such growth exponents can be understood in the framework of a logarithmic (rather than power-law) R dependence of trapping barriers. In the context of the DIM, Henley [21] and Rammal and Benoit [22] have argued that the fractal nature of domain boundaries results in a logarithmic R dependence of energy barriers. We propose that this is generally applicable and examine the implications thereof [23]. Recall that, at early times and small length scales, we expect disorder-free domain growth. Then, the appropriate logarithmic barrier-scaling form is as follows:

$$E_B(R) \simeq \epsilon \ln(1+R), \tag{6}$$

where R is measured in dimensionless units. Substituting $a(R,T) \simeq a_0 \exp(-\beta E_B)$ in Eq. (1), we obtain

$$\frac{dR}{dt} = \frac{a_0}{R} (1+R)^{-\epsilon/T}. \tag{7}$$

The solution of Eq. (7) is

$$R(t) \simeq \begin{cases} (2a_0 t)^{1/2}, & t \ll t_0, \\ \left[\left(2 + \frac{\epsilon}{T} \right) a_0 t \right]^{\theta(T,\epsilon)}, & t \gg t_0, \end{cases} \tag{8}$$

with the asymptotic growth exponent

$$\theta(T,\epsilon) = \frac{1}{2 + \epsilon/T}. \tag{9}$$

The crossover length and time can be identified by rewriting Eq. (8) in the form of Eq. (3) with

$$R_0 = \frac{1}{(2\theta)^{\theta/(1-2\theta)}},$$

$$t_0 = \frac{1}{a_0} \frac{1}{(2\theta^{2\theta})^{1/(1-2\theta)}}, \tag{10}$$

and

$$h(x) = \begin{cases} x^{1/2}, & x \ll 1, \\ x^{\theta}, & x \gg 1. \end{cases} \tag{11}$$

In our letter [14], we have shown that the growth exponent for the nonconserved RBIM is consistent with Eq. (9). Let us next discuss the implications of power-law and logarithmic barriers for domain growth with conserved kinetics.

B. Conserved case

In the absence of disorder, the domain scale obeys the Huse equation [24]

$$\frac{dR}{dt} = \frac{D_0}{R^2}, \tag{12}$$

with the solution $R(t) = (3D_0 t)^{1/3}$. The presence of disorder renormalizes the diffusion constant D_0 by an Arrhenius factor: $D(R,T) \simeq D_0 \exp(-\beta E_B)$. For logarithmic barriers as in Eq. (6), the corresponding growth equation is

$$\frac{dR}{dt} = \frac{D_0}{R^2} (1+R)^{-\epsilon/T}. \tag{13}$$

The short-time and long-time solutions of Eq. (13) are obtained as follows:

$$R(t) \simeq \begin{cases} (3D_0 t)^{1/3}, & t \ll t_0, \\ \left[\left(3 + \frac{\epsilon}{T} \right) D_0 t \right]^{\theta(T,\epsilon)}, & t \gg t_0, \end{cases} \tag{14}$$

where

$$\theta(T,\epsilon) = \frac{1}{3 + \epsilon/T}. \tag{15}$$

The crossover form of Eq. (14) is Eq. (3) with

$$R_0 = \frac{1}{(3\theta)^{\theta/(1-3\theta)}},$$

$$t_0 = \frac{1}{D_0}\frac{1}{(3\theta^{3\theta})^{1/(1-3\theta)}}, \tag{16}$$

and

$$h(x) = \begin{cases} x^{1/3}, & x \ll 1, \\ x^{\theta}, & x \gg 1. \end{cases} \tag{17}$$

Notice that the asymptotic exponent differs from that for the nonconserved case when the energy barriers are logarithmic. This should be contrasted with the HH scenario, where the asymptotic growth law is the same for the nonconserved and conserved cases [10]. This is easily seen by incorporating the HH barrier-scaling form in Eq. (12).

III. RANDOM-BOND ISING MODEL: CONSERVED KINETICS

A. Modeling and numerical details

The Hamiltonian for the RBIM is as follows:

$$\mathcal{H} = -\sum_{\langle ij \rangle} J_{ij} S_i S_j, \quad S_i = \pm 1. \tag{18}$$

For a binary (AB) mixture, the spins S_i label whether a lattice site i is occupied by an A atom (say, $S_i=+1$) or a B atom ($S_i=-1$). We consider the case where the spins are placed on an L^2 square lattice with periodic boundary conditions. We introduce quenched disorder in the exchange coupling J_{ij}, corresponding to immobile impurities in a binary mixture. The J_{ij}'s have a uniform distribution on the interval $[1-\epsilon/2, 1+\epsilon/2]$, where ϵ quantifies the amount of disorder. The limit $\epsilon=2$ corresponds to maximum disorder, and $\epsilon=0$ corresponds to the pure case. (We confine ourselves to the case where the exchange couplings are always ferromagnetic, $J_{ij} \geqslant 0$.) The subscript $\langle ij \rangle$ in Eq. (18) denotes a sum over nearest-neighbor pairs only. For the pure case, $T_c^{\text{pure}} \simeq 2.269$ for a $d=2$ square lattice. Since the average coupling strength is $\langle J_{ij} \rangle = 1$, as in the pure case, the critical temperature remains almost unaltered, $T_c \in [2.0, 2.269]$ [25]. Assigning random initial orientations to each spin, we rapidly quench the system to $T < T_c$. The initial condition corresponds to a critical quench, with 50% A (up) and 50% B (down).

The Ising model has no intrinsic dynamics as the commutator of the spin variables and the Hamiltonian is identically zero. Therefore, we introduce stochastic dynamics by placing the system in contact with a heat bath. The resultant dynamical model is referred to as a *kinetic Ising model*. The appropriate stochastic kinetics for a binary mixture is Kawasaki spin-exchange or conserved kinetics, where a randomly selected spin S_i is exchanged with a randomly chosen neighbor, $S_i \leftrightarrow S_j$. The spin exchange is accepted with probability

$$W = \begin{cases} \exp(-\beta \Delta\mathcal{H}) & \text{for } \Delta\mathcal{H} \geqslant 0, \\ 1 & \text{for } \Delta\mathcal{H} \leqslant 0, \end{cases} \tag{19}$$

where $\Delta\mathcal{H}$ is the change in energy resulting from the spin exchange:

$$\Delta\mathcal{H} = (S_i - S_j)\left(\sum_{L_i \neq j} J_{iL_i} S_{L_i} - \sum_{L_j \neq i} J_{jL_j} S_{L_j} \right). \tag{20}$$

In Eq. (20), L_i refers to the nearest neighbors of lattice site i. A single Monte Carlo step (MCS) corresponds to attempted updates of L^2 spins. A naive implementation of the Kawasaki model is numerically demanding, and it has proven notoriously difficult to access the asymptotic LS growth regime in the pure case [26,27]. A number of accelerated algorithms have been proposed in the literature [28]—we employ the so-called *continuous-time algorithm*. In this approach, a list of oppositely oriented spins is prepared from the lattice configuration. Then, a pair is selected randomly from the list, and is exchanged according to Eq. (19). In each trial, time is advanced by $\Delta t = 1/n_t$, where n_t is the total number of antialigned spin pairs at time t. After each exchange, the list is updated. This algorithm works particularly efficiently at low temperatures, where bulk domains are strongly enriched in one component.

The segregating system is usually characterized by studying the time dependence of the correlation function:

$$C(\vec{r},t) = \frac{1}{N}\sum_{i=1}^{N} [\langle S_i(t) S_{i+\vec{r}}(t) \rangle - \langle S_i(t) \rangle \langle S_{i+\vec{r}}(t) \rangle]_{\text{av}}, \tag{21}$$

which measures the overlap of the spin configuration at distance $\vec{r}$. Here, $[\cdots]_{\text{av}}$ indicates an average over different realizations of the bond disorder, and $\langle \cdots \rangle$ denotes a thermal average, i.e., an average over different initial configurations and realizations of the thermal noise. Typically, the growth process is isotropic and characterized by a unique length scale $R(t)$. In that case, the correlation function has a dynamical-scaling form [29]

$$C(\vec{r},t) = g\left(\frac{r}{R}\right), \tag{22}$$

where $g(x)$ is the scaling function.

The characteristic size $R(t)$ is defined from the correlation function as the distance over which it decays to (say) zero or half its maximum value. There are a number of different definitions of the length scale, but these are all equivalent in the scaling regime. Subsequently, we will present results for the correlation function and the domain growth law.

B. Numerical results

In Fig. 1, we show evolution pictures for the conserved RBIM after a critical quench from $T=\infty$ to 1.0. We show snapshots at $t=10^7$ MCS for $\epsilon=0$ (pure case), and $\epsilon=1$, 2. The domains have been identified by calculating the time average for each spin:

$$m_i = \frac{1}{\Delta}\sum_{t=t_i}^{t_f} S_i(t), \tag{23}$$

within a suitable time window $\Delta = t_f - t_i$. This averaging procedure reduces the excess noise due to finite-temperature fluctuations, and enables the clear identification of domains. The evolution pictures shown subsequently are also obtained

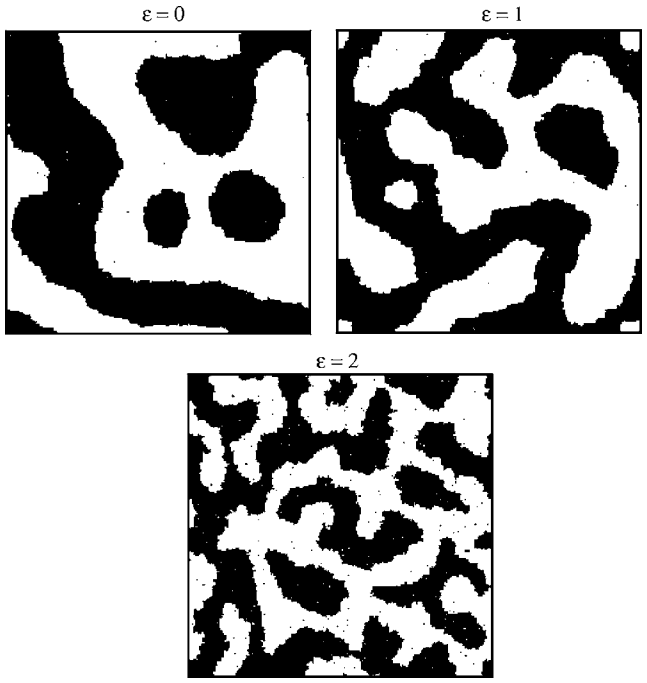

FIG. 1. Domain growth in the RBIM with Kawasaki kinetics. We show evolution pictures at $t=10^7$ MCS for a 256^2 lattice, after a quench from $T=\infty$ to 1.0. Regions with $m_i>0$ (A rich) are marked black, and regions with $m_i<0$ (B rich) are unmarked. The mixture has a critical composition with 50% A and 50% B. The snapshots correspond to different disorder amplitudes: $\epsilon=0$ (pure case) and $\epsilon=1$, 2.

using the same method. It is clear from the snapshots in Fig. 1 that the evolution is slower for higher amplitudes of disorder. This will be quantified via the corresponding domain growth laws.

Next, we consider the scaled correlation-function data $[C(r,t)$ vs $r/R]$ for the morphologies in Fig. 1. Our statistical data for the RBIM are obtained on $d=2$ lattices of size 512^2 (with $T=1.0$ and ϵ being varied), and 256^2 (with $\epsilon=2$ and T being varied). In order to improve the statistics, we averaged within a finite time window around each data point. Further, the data were obtained as an average over 32 independent initial conditions for both the spin and disorder configurations. The length scale R is defined as the first zero crossing of the correlation function. We have confirmed that $C(r,t)$ exhibits dynamical scaling [as in Eq. (22)] for different disorder amplitudes and quenches to different values of T. In Fig. 2, we show that the scaling function is independent of the disorder amplitude. This has also been demonstrated in earlier studies of phase separation in disordered systems [10,13]. In physical terms, the universality of the scaling function means that the morphologies are equivalent, regardless of the disorder amplitude. (This was already suggested by the snapshots in Fig. 1.) The typical transverse displacement of interfaces due to disorder roughening is $L^{\zeta/(2-\zeta)}$, where ζ is the roughening exponent [5]. At late times, one has $L \gg L^{\zeta/(2-\zeta)}$, because $\zeta<1$ above the lower critical dimension. (If $\zeta>1$, disorder-induced roughening would destroy long-range order in the system.) Thus, in the asymptotic regime, the roughness is irrelevant compared to the domain

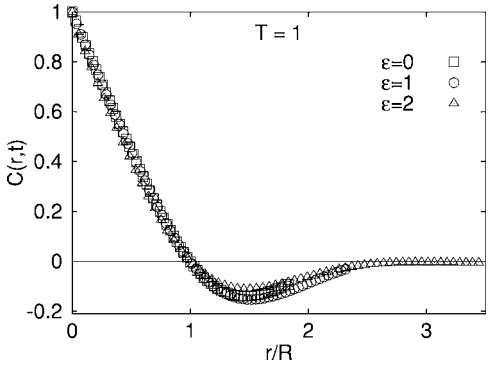

FIG. 2. Scaling plot of the correlation function for the evolution depicted in Fig. 1. We plot $C(r,t)$ vs r/R at $t=10^7$ MCS for disorder amplitudes $\epsilon=0$ (pure case) and $\epsilon=1$, 2. The length scale is defined as the first zero crossing of $C(r,t)$.

size. Therefore, the evolution morphologies and their statistical properties should be independent of disorder at late times.

Next, let us investigate the time dependence of the domain size. First, we study $R(t)$ vs t for quenches to different temperatures. In Fig. 3, we undertake a direct test of the HH growth law in Eq. (2) by plotting $R^{1/4}$ vs $\ln t$ for $\epsilon=2$ and different T values. Recall that $\psi=1/4$ in $d=2$ according to the HH argument, and the corresponding plot in Fig. 3 should be linear in the asymptotic regime. However, the plot exhibits continuous curvature and is not consistent with the HH growth law. It may be argued that these data correspond to a crossover regime which is a prelude to the HH growth law. In this context, we have attempted to fit the data to the conserved counterpart of the crossover function in Eq. (3). However, in accordance with our results for the nonconserved RBIM [14], there are important points of disagreement between the numerical data and the scaling function. We will discuss this issue further in Sec. IV B.

Finally, we have also fitted our data for $R(t)$ vs t to the *logarithmic* function $\ln t=aR^x+b$. In general, this function does not give a reasonable fit to the data. Even for these poor fits, the exponent x is strongly dependent on the temperature, at variance with the prediction of a universal growth law. A similar observation has been made in the experiments of Ikeda *et al.* [18], though these were performed on random

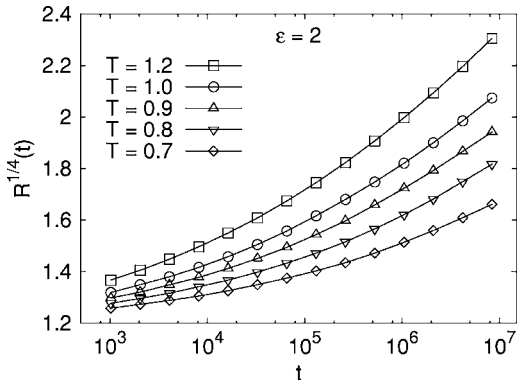

FIG. 3. Plot of $R^{1/4}$ vs t (on a log-linear scale) for $\epsilon=2$ and different quench temperatures: $T=0.7$, 0.8, 0.9, 1.0, 1.2.

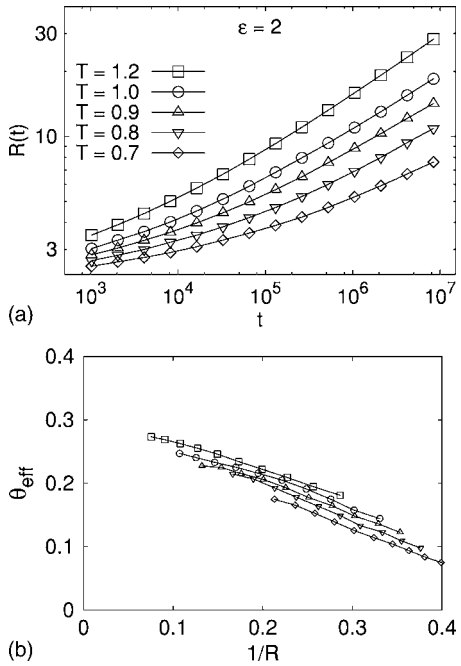

FIG. 4. (a) Plot of R vs t (on a log-log scale) for the length-scale data shown in Fig. 3. (b) Plot of $\theta_{\text{eff}}=d(\ln R)/d(\ln t)$ vs R^{-1} for the data in (a).

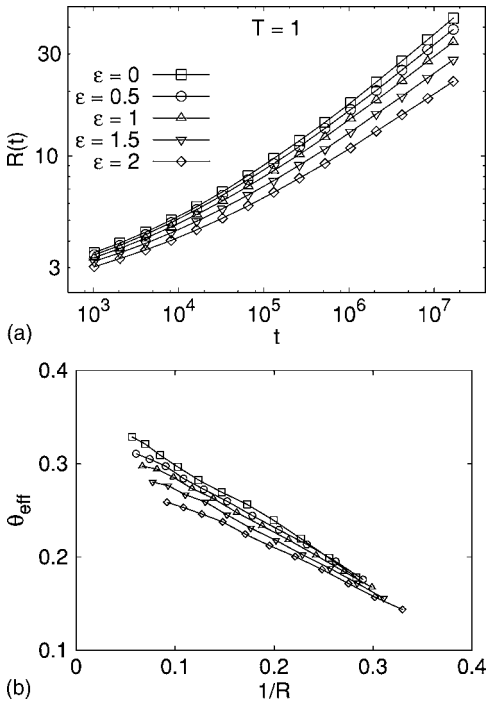

FIG. 5. (a) Plot of R vs t (on a log-log scale) for $T=1.0$ and different disorder amplitudes: $\epsilon=0$ (pure case), and $\epsilon=0.5$, 1.0, 1.5, 2.0. (b) Plot of $\theta_{\text{eff}}=d(\ln R)/d(\ln t)$ vs R^{-1} for the data in (a).

magnets, rather than disordered mixtures. As a matter of fact, Ikeda *et al.* and Likodimos *et al.* [19,20] have argued that their experimental data for domain growth in disordered systems are described by a power law with a temperature-dependent exponent rather than the HH growth law. We have made a similar observation in our MC studies of the nonconserved RBIM [14]. Let us examine the length-scale data for the conserved RBIM from this perspective.

In Fig. 4(a), we plot R vs t from Fig. 3 on a log-log scale. This plot does not show an extended linear regime on the time scale of our simulation. However, it is known that there is an extended preasymptotic growth regime in the conserved case without disorder [24,26,27], which complicates the observation of the LS growth regime in MC simulations. Further, the slight upward curvature in the log-log plot suggests that the growth law cannot be slower than a power law, at variance with the HH result. In the pure case, Huse [24] has suggested that the asymptotic exponent may be obtained by extrapolating the graph of the effective exponent $\theta_{\text{eff}}=d(\ln R)/d(\ln t)$ vs R^{-1}. We apply a similar technique to the disordered case, and query whether the resultant exponents are consistent with the scenario in Sec. II B [cf. Eq. (15)]. In Fig. 4(b), we plot θ_{eff} vs R^{-1} for the data in Fig. 4(a). The plots in Fig. 4(b) can be smoothly extrapolated to $R^{-1}=0$ ($R=\infty$) to determine $\theta=\theta_{\text{eff}}(\infty)$, which depends on T.

Next, we consider R vs t at fixed temperature as the disorder amplitude is varied. Again, we find that our data are not consistent with either the HH scenario or even logarithmic growth. In Fig. 5(a), we plot R vs t on a log-log scale for different ϵ values. The corresponding plots of θ_{eff} vs R^{-1} are shown in Fig. 5(b). In this case, the asymptotic exponent depends on the disorder amplitude. Notice that we have also shown data for the pure case ($\epsilon=0$) in Fig. 5(a). We do not see an extended linear regime even in this case. However, the corresponding plot of θ_{eff} vs R^{-1} in Fig. 5(b) extrapolates to the well-known LS value, $\theta\simeq 0.33$.

In Sec. II B, we have seen that a logarithmic barrier scaling results in power-law growth with varying exponents. We would like to test whether the asymptotic exponents are consistent with the result in Eq. (15). In Figs. 6(a) and 6(b), we plot θ^{-1} vs T^{-1} and ϵ, respectively. The resultant linear plots strongly support the logarithmic barrier-scaling scenario.

IV. DILUTE ISING MODEL

A. Modeling and numerical details

Next, we turn our attention to the DIM, where bond disorder is introduced by diluting the spins on the lattice. The corresponding Hamiltonian is

$$\mathcal{H}=-J\sum_{\langle ij\rangle}\rho_i\rho_j S_i S_j, \quad S_i=\pm 1, \tag{24}$$

with $J>0$. In Eq. (24), the ρ_i's are quenched, uncorrelated random variables with the probability distribution

$$P(\rho)=p\,\delta_{\rho,1}+(1-p)\,\delta_{\rho,0}. \tag{25}$$

For a ferromagnet, $\rho_i=0$ implies that the magnetic atom at i is replaced by a nonmagnetic impurity. In the context of an AB mixture, $\rho_i=0$ corresponds to an immobile (noninteracting) impurity at site i. Thus, there is no exchange interaction between the atom at site i and its nearest neighbors. The distinguishing feature of the DIM (in contrast to the RBIM discussed in Sec. III) is the existence of a percolation threshold $p=p_c$ [30]. For $p=1$, the system is pure and shows fer-

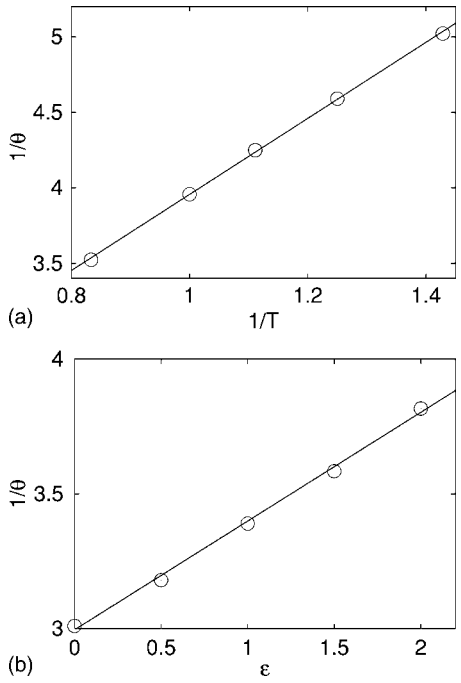

FIG. 6. (a) Exponent $1/\theta$ vs $1/T$ for the data in Fig. 4. The solid line denotes the best linear fit to the data. (b) Exponent $1/\theta$ vs ϵ for the data in Fig. 5.

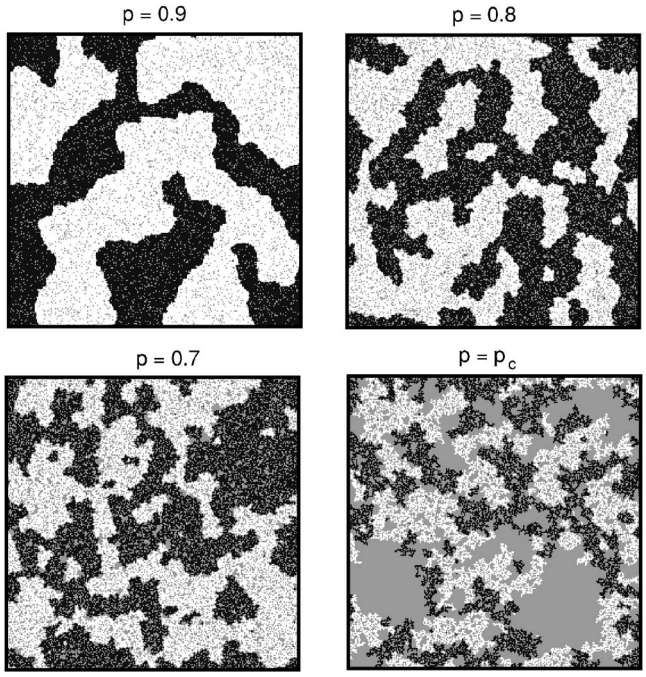

FIG. 7. Domain growth in the DIM with Glauber kinetics. We show evolution pictures at $t=10^6$ MCS for a 256^2 corner of a 512^2 lattice, after a quench from $T=\infty$ to 0.5. The snapshots correspond to different site occupation probabilities: $p=0.9$, 0.8, 0.7, 0.593 (p_c). The up and down spins are marked black and white, respectively. The missing spins are marked gray.

romagnetic order at $T<T_c(p=1)$. The critical temperature $T_c(p)$ diminishes as p is decreased and becomes 0 at $p=p_c$. (For a $d=2$ square lattice, $p_c \simeq 0.593$.) For $p<p_c$, there are no infinite clusters of magnetic atoms which span the system, i.e., there is no long-range order. For weak disorder ($p \simeq 1$), the kinetic DIM is analogous to the kinetic RBIM. However, for smaller values of p, connectivity effects become important and may change the nature of domain growth. We are particularly interested in the ordering dynamics of the DIM for $p \simeq p_c$.

In this section, we focus on two systems.

(a) The DIM with nonconserved (Glauber) kinetics, which models the ordering dynamics of a dilute ferromagnet. In an MC simulation of Glauber kinetics, a randomly-chosen spin S_i is flipped to $-S_i$ and the system is evolved according to the prescription in Eq. (19).

(b) The DIM with conserved (Kawasaki) kinetics, which models the segregation kinetics of a dilute binary mixture. In this case, we use the continuous-time algorithm described in Sec III A.

The initial conditions for our MC simulations are prepared as follows. We dilute the sites of an L^2 lattice with probability $1-p$. (These sites remain fixed during the evolution.) Then, up and down spins are randomly distributed on the remaining sites with a zero net magnetization, mimicking the high-temperature disordered configuration before the quench.

B. Nonconserved kinetics

In Fig. 7, we show evolution snapshots at $t=10^6$ MCS for $T=0.5$ and $p=0.9$, 0.8, 0.7, 0.593 (p_c). Notice that $T_c(p=0.7) \simeq 1.04$ for the $d=2$ DIM [31], so that $T=0.5$ lies below the critical temperature for all the values of p other than $p=p_c$, where $T_c(p_c)=0$. (Unfortunately, it is difficult to do MC simulations at $T=0$, as the system is rapidly trapped in a metastable state.) As expected, the domain size at a fixed time diminishes with increase in disorder. In the case of evolution on the backbone of a percolating cluster, the morphology consists of a network of islands (compact well-connected regions) linked by just a single bond. As time progresses, these islands become fully magnetized, but they cannot influence the evolution of their neighbors. For this reason, domain growth becomes very slow at $p=p_c$. Further, as $T>T_c(p_c)$, domain growth is arrested when the length scale saturates at the equilibrium correlation length $\xi_{\rm eq}(T) \to \infty$ as $T \to 0$.

Let us next focus on the properties of these evolution morphologies. Our statistical data for the nonconserved DIM are obtained using 512^2 systems, by averaging over 50 independent initial conditions and disorder configurations. We have confirmed that the evolution of the nonconserved DIM shows dynamical scaling. In Fig. 8, we demonstrate the disorder independence of the scaled correlation function. Here, we plot $C(r,t)$ vs r/R at $t=10^6$ MCS for $p=0.8, 0.7, p_c$, and compare the plots with the corresponding data for the pure case ($p=1$). In this case, the domain size is defined as the r value where the correlation function decays to half its maximum value. Notice that the scaling function for $p=p_c$ is analogous to that for higher values of p, and there are no distinctive signatures of the percolation cluster.

Next, consider the time dependence of the length scale. We first study the case with $p=0.8$ and varying T values. In

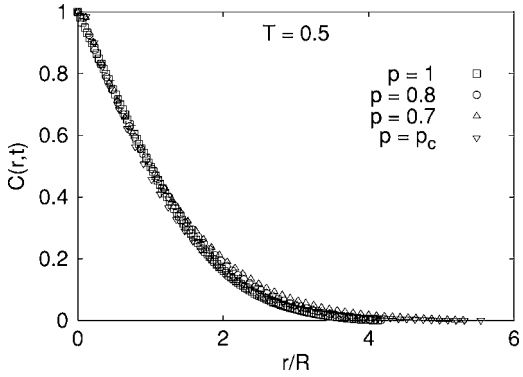

FIG. 8. Scaling plot of the correlation function for the evolution depicted in Fig. 7. We plot $C(r,t)$ vs r/R at $t=10^6$ MCS for occupation probability $p=0.8,0.7,p_c$. We also show data for the pure case ($p=1$) at $t=10^3$ MCS, obtained for a 1024^2 system.

Fig. 9, we attempt to fit our length-scale data to the HH crossover function in Eqs. (3)–(5). We record the following points of disagreement with the HH scaling behavior.

(a) The short-time behavior is not described well by Eq. (5), where $h_1(x) \sim x^{1/2}$.

(b) The asymptotic behavior in Eq. (5) [denoted by the curve $h_2(x)$ in Fig. 9] does not fit the scaling curve well even for the largest times.

(c) The temperature dependence of the crossover length $R_0(T)$ and the crossover time $t_0(T)$ is stronger than a power law (see inset of Fig. 9), which is incompatible with Eqs. (2) and (4). The parameter a_0 in Eq. (2) is proportional to the surface tension, and is expected to decrease with increasing temperature. Therefore, t_0 can be expected to increase faster than T^8, but its T dependence turns out to be much too strong: note that t_0 in the inset of Fig. 9 varies over 20 decades when T varies over only half a decade from 0.4 to 0.8. We do not see why the surface tension should have such a strong T dependence.

Based on observations (a)–(c), we believe that the data in Fig. 9 are inconsistent with the HH growth law.

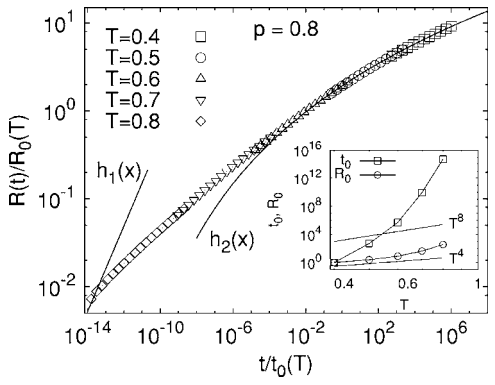

FIG. 9. Scaling plot to test the crossover function in Eqs. (3)–(5). For each temperature T, the values for $R_0(T)$ and $t_0(T)$ have been chosen to obtain a smooth scaling curve $h(x)$. The functions $h_1(x) \propto x^{1/2}$ and $h_2(x) \propto (\ln x)^4$ represent the expected asymptotic behavior for $x \ll 1$ and $x \gg 1$, respectively. The inset shows the temperature dependence of the fit values $R_0(T)$ and $t_0(T)$, and their expected T dependence, which is T^4 and T^8, respectively.

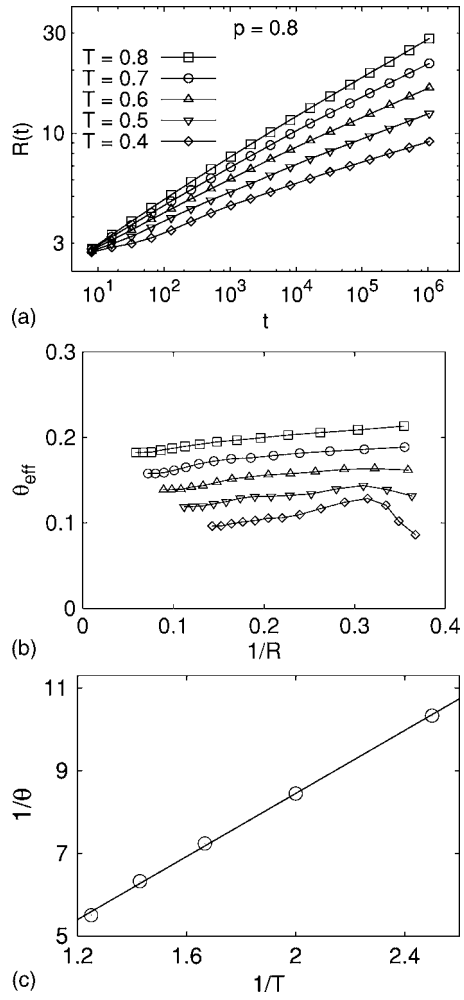

FIG. 10. (a) Plot of R vs t (on a log-log scale) for the nonconserved DIM with $p=0.8$ and temperatures $T=0.4$, 0.5, 0.6, 0.7, 0.8. (b) Plot of $\theta_{\text{eff}}=d(\ln R)/d(\ln t)$ vs R^{-1} for the data in (a). (c) Plot of θ^{-1} vs T^{-1} for the data in (a).

In Fig. 10(a), we plot R vs t on a log-log scale for $p=0.8$ and $T=0.8$, 0.7,0.6, 0.5, $0.4 < T_c(p=0.8) \simeq 1.5$. The corresponding plots of θ_{eff} vs R^{-1} are shown in Fig. 10(b). These show an extended flat regime, making it relatively simple to estimate the exponent. As in the case of the RBIM, our data are consistent with power-law growth with a variable exponent. In Fig. 10(c), we plot $\theta(T,p)^{-1}$ vs T^{-1}–the linear behavior is consistent with Eq. (9). (See Ref. [14] for similar results for the nonconserved RBIM.)

Finally, in Fig. 11(a), we plot R vs t at percolation ($p=p_c$) and $T=0.7$, 0.6, 0.5, $0.4 > T_c(p_c)=0$. Recall that the domain scale saturates to $\xi_{\text{eq}}(T)$ in this case, with an earlier crossover for higher T. On the time scale of our simulation, the data for $T=0.7$ have saturated, and those for $T=0.6$ are beginning to bend over. This is reflected in Fig. 11(b), which shows θ_{eff} vs R^{-1}. The exponent θ is estimated from the flat portion of these curves, and we plot θ^{-1} vs T^{-1} in Fig. 11(c).

C. Conserved kinetics

We have performed a similar study of the DIM with Kawasaki kinetics. In this case, the time scale of growth is

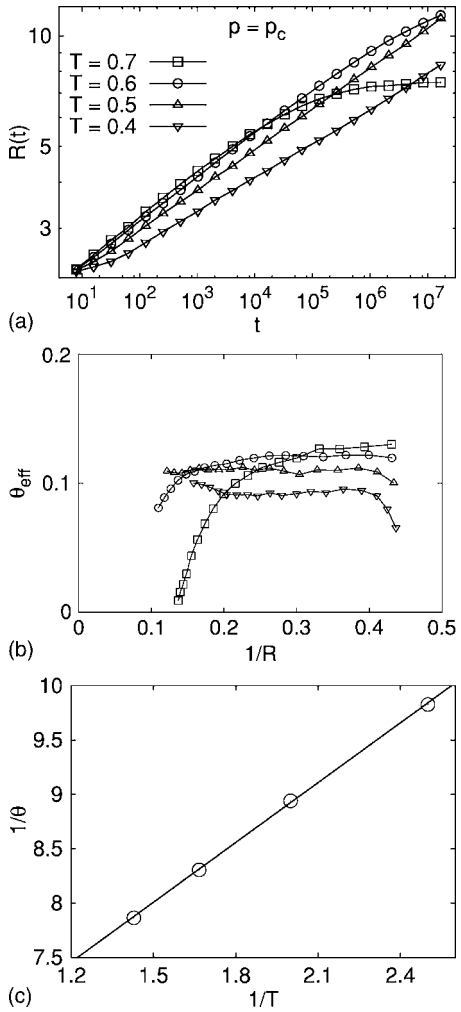

FIG. 11. Analogous to Fig. 10 but for $p=p_c$.

considerably slower than for the nonconserved case. The typical evolution morphologies at $t=10^7$ MCS (after a critical quench from $T=\infty$ to 0.5) are shown in Fig. 12. As in the earlier cases, we will show results for the correlation function and the growth law. The statistical data shown here were obtained on a 256^2 lattice as an average over 32 independent configurations.

In Fig. 13, we plot $C(r,t)$ vs r/R at $t=10^7$ MCS for the pure case, and different values of the dilution. [The length scale is obtained from the first zero of $C(r,t)$.] Again, the scaling function is approximately independent of the amount of dilution. Next, we focus on the time dependence of the length scale. In Fig. 14(a), we plot R vs t for $p=0.8$ and various values of T. Again, we estimate the asymptotic exponent from plots of θ_{eff} vs R^{-1} (not shown here). In Fig. 14(b), we plot the corresponding θ^{-1} vs T^{-1}.

Figure 15 is analogous to Fig. 14, but for $p=p_c$. As the growth is much slower than in the nonconserved case, we do not see a crossover to saturation for $p=p_c$ on the time scale of our simulations. Once again, the exponents are consistent with the logarithmic barrier-scaling scenario.

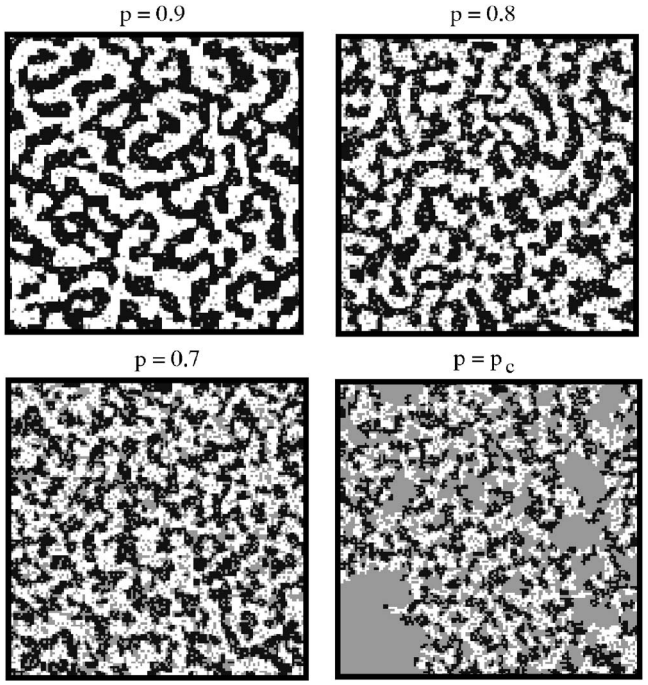

FIG. 12. Domain growth in the DIM with Kawasaki kinetics. We show evolution pictures at $t=10^7$ MCS for a 128^2 corner of a 256^2 lattice, after a quench from $T=\infty$ to 0.5. The snapshots correspond to different site occupation probabilities: $p=0.9$, 0.8, 0.7, 0.593 (p_c). The color coding is the same as in Fig. 7.

V. SUMMARY AND DISCUSSION

Let us conclude this paper with a summary and discussion of the results presented here and in our earlier letter [14]. We have undertaken comprehensive Monte Carlo simulations of domain growth in Ising systems with quenched disorder. These studies are based on kinetic Ising models with either nonconserved (Glauber) spin-flip kinetics or conserved (Kawasaki) spin-exchange kinetics. The nonconserved case models ordering dynamics in random magnets, and the conserved case models segregation kinetics in disordered binary mixtures. We have studied domain growth for two classes of disordered systems.

(a) The random-bond Ising model, where the ex-

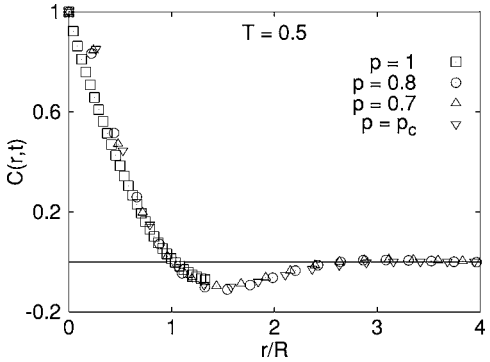

FIG. 13. Scaling plot of the correlation function for the evolution depicted in Fig. 12. We plot $C(r,t)$ vs r/R at $t=10^7$ MCS for occupation probability $p=1$ (pure case) and 0.8, 0.7, p_c.

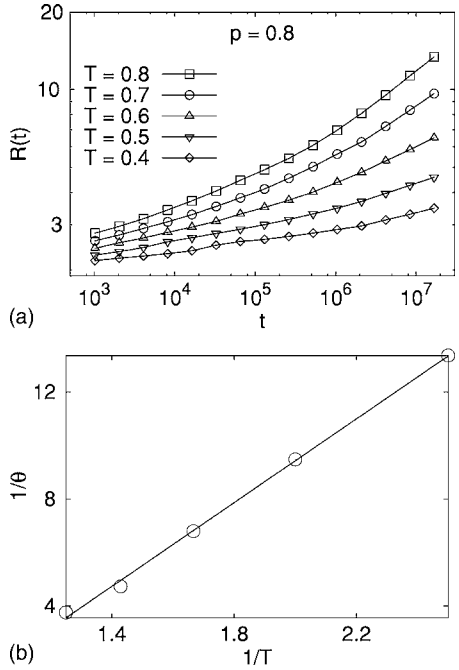

FIG. 14. (a) Plot of R vs t (on a log-log scale) for the conserved DIM with $p=0.8$ and $T=0.4$, 0.5, 0.6, 0.7, 0.8. (b) Plot of θ^{-1} vs T^{-1} for the data in (a).

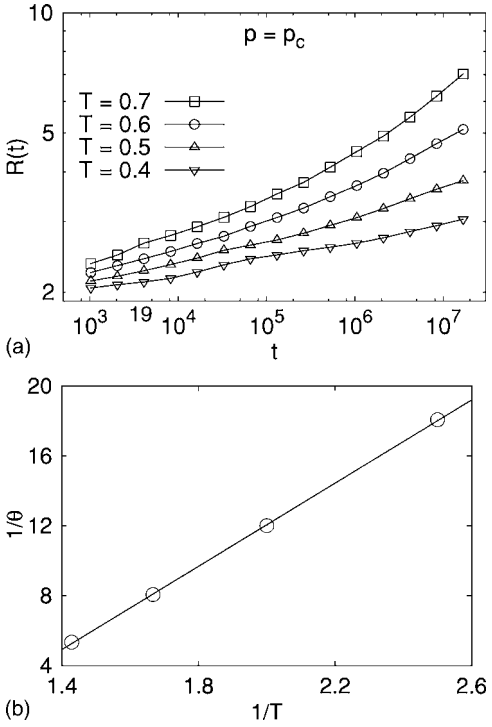

FIG. 15. Analogous to Fig. 14, but for $p=p_c$.

change interaction has a uniform distribution on the interval $[1-\epsilon/2, 1+\epsilon/2]$, $\epsilon<2$. In this case, the critical temperature $T_c(\epsilon)$ remains approximately unchanged.

(b) The dilute Ising model, where the exchange interaction is randomized by the dilution of magnetic atoms with nonmagnetic impurities. In this case, the critical temperature $T_c(p)$ ranges from $T_c(p=1)\simeq 2.269$ (in $d=2$) to $T_c(p=p_c)=0$ ($p_c\simeq 0.593$ in $d=2$). Both classes of disorder are of considerable experimental relevance.

The general framework for understanding coarsening in disordered systems is as follows. At early times, the domain sizes are small and domain growth is unaffected by disorder. At late times, the domain boundaries are trapped by disorder sites, and asymptotic growth proceeds via thermally activated hopping over disorder barriers. Clearly, the asymptotic growth law depends critically on the length-scale dependence of the disorder barrier E_B. In this context, an important study is due to Huse and Henley [5]. In the HH scenario, the disorder barriers have a power-law dependence on the domain size, $E_B\sim R^{\psi}$. These result in a logarithmic domain growth law in the asymptotic regime. We find that our MC results are not in agreement with the HH scenario. Rather, our results are consistent with power-law growth with an exponent θ which depends on the temperature T and the disorder amplitude ϵ. This is in agreement with a number of experiments [18–20], and early simulations of droplet shrinking in disordered systems by Oh and Choi [7]. This scenario arises naturally in the context of logarithmic energy barriers, and the corresponding functional dependence of $\theta(T,\epsilon)$ is in excellent agreement with our numerical results.

Our results provide a framework for the analysis of experiments and simulations on domain growth in disordered magnets and binary mixtures. We hope that our study will motivate fresh experimental studies of this important problem. In particular, there is a paucity of experimental results on phase separation in disordered mixtures.

ACKNOWLEDGMENT

This work was financially supported by the Deutsche Forschungsgemeinschaft (DFG) SFB277.

[1] A. J. Bray, Adv. Phys. **43**, 357 (1994).

[2] K. Binder and P. Fratzl, in *Materials Science and Technology*, edited by G. Kostorz (Wiley-VCH, Weinheim, 2001), Vol. 5, p. 409.

[3] A. Onuki, *Phase Transition Dynamics* (Cambridge University Press, Cambridge, U. K., 2002).

[4] S. Dattagupta and S. Puri, *Dissipative Phenomena in Condensed Matter: Some Applications* (Springer-Verlag, Berlin, 2004).

[5] D. A. Huse and C. L. Henley, Phys. Rev. Lett. **54**, 2708 (1985).

[6] G. S. Grest and D. J. Srolovitz, Phys. Rev. B **32**, 3014 (1985); D. J. Srolovitz and G. S. Grest, *ibid.* **32**, 3021 (1985).

[7] J. H. Oh and D.-I. Choi, Phys. Rev. B **33**, 3448 (1986).

[8] D. Chowdhury, M. Grant, and J. D. Gunton, Phys. Rev. B **35**, 6792 (1987); B. Biswal, S. Puri, and D. Chowdhury, Physica A

229, 72 (1996).
[9] S. Puri, D. Chowdhury, and N. Parekh, J. Phys. A **24**, L1087 (1991).
[10] S. Puri and N. Parekh, J. Phys. A **25**, 4127 (1992).
[11] H. Hayakawa, J. Phys. Soc. Jpn. **60**, 2492 (1991); T. Iwai and H. Hayakawa, *ibid.* **62**, 1583 (1993).
[12] A. J. Bray and K. Humayun, J. Phys. A **24**, L1185 (1991).
[13] M. F. Gyure, S. T. Harrington, R. Strilka, and H. E. Stanley, Phys. Rev. E **52**, 4632 (1995).
[14] R. Paul, S. Puri, and H. Rieger, Europhys. Lett. **68**, 881 (2004).
[15] Z. W. Lai, G. F. Mazenko, and O. T. Valls, Phys. Rev. B **37**, 9481 (1988).
[16] D. Forster, D. R. Nelson, and M. J. Stephen, Phys. Rev. A **16**, 732 (1977).
[17] D. A. Huse, C. L. Henley, and D. S. Fisher, Phys. Rev. Lett. **55**, 2924 (1985).
[18] H. Ikeda, Y. Endoh, and S. Itoh, Phys. Rev. Lett. **64**, 1266 (1990).
[19] V. Likodimos, M. Labardi, and M. Allegrini, Phys. Rev. B **61**, 14440 (2000).
[20] V. Likodimos, M. Labardi, X. K. Orlik, L. Pardi, M. Allegrini, S. Emonin, and O. Marti, Phys. Rev. B **63**, 064104 (2001).
[21] C. L. Henley, Phys. Rev. Lett. **54**, 2030 (1985).
[22] R. Rammal and A. Benoit, Phys. Rev. Lett. **55**, 649 (1985).
[23] A logarithmic R dependence of energy barriers was also proposed in the context of spin glasses; see H. Rieger, J. Phys. A **26**, L615 (1993); J. Kisker, L. Santen, M. Schreckenberg, and H. Rieger, Phys. Rev. B **53**, 6418 (1996). For spin glasses, it also leads to an algebraic growth law with temperature-dependent exponents.
[24] D. A. Huse, Phys. Rev. B **34**, 7845 (1986).
[25] We determined the critical temperature $T_c(\epsilon)$ in the standard way usung finite size scaling of the data for the Binder cumulant computed via equilibrium Monte Carlo simulations. T_c decreases monotonically from 2.269 for $\epsilon=0$ to 2.0 for $\epsilon=2$.
[26] J. G. Amar, F. E. Sullivan, and R. D. Mountain, Phys. Rev. B **37**, 196 (1988).
[27] J. F. Marko and G. T. Barkema, Phys. Rev. E **52**, 2522 (1995).
[28] M. E. Newman and G. T. Barkema, *Monte Carlo Methods in Statistical Physics* (Clarendon Press, Oxford, 1999).
[29] K. Binder and D. Stauffer, Phys. Rev. Lett. **33**, 1006 (1974); Z. Phys. B **24**, 406 (1976).
[30] D. Stauffer, Phys. Rep. **54**, 1 (1979);D. Stauffer, *Introduction to Percolation Theory* (Taylor and Francis, London, 1985).
[31] W. Y. Ching and D. L. Huber, Phys. Rev. B **13**, 2962 (1976).